The Sound from Underwater Explosions

David R. Dall'Osto, Peter H. Dahl, and N. Ross Chapman

Introduction

Explosives have played a prominent role in the history of underwater acoustics. In fact, much of our understanding of sound propagation in the ocean was developed from analysis of data from experiments at sea using explosive charges. Some of the early research was done under highly dangerous conditions during World War II (WWII) when experiments needed to be carried out in the very waters patrolled by enemy submarines. Many lasting innovations were developed out of these wartime studies, including cutting edge air-dropped radio buoys with hydrophones that were critical to mitigating submarine threats (Muir and Bradley, 2016).

Another lasting example of these early efforts was the development of a dense hydrophone infrastructure initially designed for rescue of pilots and aircrew lost at sea. This system, called the SOund Fixing And Ranging (SOFAR) system, was developed after the surprising discovery of the deep ocean sound channel, the SOFAR channel. This sound channel exists due to the natural structure of sound speed in the ocean. Sound speed is higher in the upper ocean due to solar warming and at great depths in the lower ocean due to the extreme hydrostatic pressure. A minimum sound speed is thus established at middle ocean depths. This natural structure of sound speed creates an acoustic lens in the ocean that enables sound originating in the channel to propagate to very long ranges.

As a consequence, a small explosion detonated at a depth near the sound speed minimum can be detected tens of thousands of kilometers away. During WW II, a system was developed where downed pilots would drop a small explosive charge, using a reference table to first set an appropriate depth in the SOFAR channel for the detonation. Through detection and timing of the sound received at multiple listening stations, operators would generate a fix on the aircrew's position to dispatch a search and rescue. Although satellite technology has replaced this method, these early efforts identified the feasibility and utility of long-range hydroacoustic networks. As an aside, it was not only oceanographers who used the SOFAR channel but is also used by baleen whales to communicate across the world's oceans (Schulze et al., 2022).

Beyond use of the SOFAR channel, there have been many other important contributions to understanding the oceans using explosives. In this article, we discuss how their use continues to add to our understanding of underwater acoustics. We focus on the sound emanated from a standard naval ordinance called Signal, Underwater Sound (SUS) charges that have been used for over 60 years and are still used in underwater acoustic research today.

Signal, Underwater Sound Charges

SUS charges were mass produced in the United States throughout the 1960s to the 1990s to support antisubmarine warfare (ASW). In a typical ASW mission, aircraft and ships would first set out a network of listening buoys. After the network was deployed, SUS charges would be dropped (typically from an airplane) into the water and operators would analyze the sound, specifically listening for reflections of the shockwave from the submarine's hull. If an echo was heard (a contact!), the process would repeat to track the submarine. Such operations ceased in the 1960s as explosive SUS charges were phased out in favor of less dangerous (and more effective) electronic variants as sound sources.

Small explosives, like SUS charges, are appealing for use in experiments at sea because their deployment is relatively straightforward from ships or aircraft, and they provide

https://doi.org/10.1121/AT.2023.19.1.12

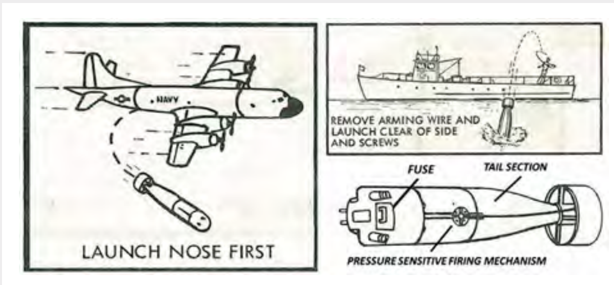

Figure 1. *Images from the instructions and warnings included with signal, underwater sound (SUS) charges manufactured in the 1960s.* ***Left:*** *SUS charge deployment from an aircraft.* ***Top right:*** *deployment from a surface ship.* ***Bottom right:*** *detail of a SUS charge, with its three sections: the "fuse," the "pressure-sensitive firing mechanism," and the aerodynamic "tail section" that is packed with a high-energy (HE) explosive. A typical operational SUS charge (Mk82) contains 0.82 kg of HE explosive, whereas a practice charge (Mk64) only contains 31 g of HE in its fuse and has an inert tail section. Image credit: NAVAIR DWG 695611.*

strong broadband, or wide-frequency-range, signals, with appreciable energy at frequencies well below 1,000 Hz. Somewhat conveniently, a supply of explosive SUS ordinance is still available and used in present day research.

Figure 1 shows a 1960s era instruction/warning sheet included with the SUS charges that were recently used in experiments off the New Jersey coast. We use measurements of a "practice SUS charge" (model Mk64) and an "operational SUS charge" (model Mk82) to illustrate the sequence of events in the acoustic signal and to demonstrate the fundamental scaling laws universal to all underwater explosions.

Pressure Signal Sequence of an Underwater Explosive Source Measured at Close Range

The initial sound from an underwater explosion radiates as a shockwave, producing a near instantaneous rise in pressure that can be hundreds of times greater than the ambient hydrostatic pressure. The shockwave appears as a sharp spike in hydrophone measurements made relatively close to the source. The peak pressure of the shockwave from a practice SUS (Mk64) charge at a 12 m range is about 0.73 MPa (see **Figure 2**, *top*), and for the operational SUS (Mk82) charge at a 70 m range is about 0.33 MPa (**Figure 2**, *bottom*). Although the operational SUS charge contains 26 times the amount of explosive, the smaller practice charge produces a higher peak pressure at the recording hydrophone because it was measured at a closer range.

After the initial sudden rise in pressure when the shock impulse arrives at the hydrophone, the pressure decays quickly and returns to the ambient level within a few milliseconds. The initial part of the decay is generally modeled as being exponential. However, high-resolution data of the shock impulse reveals that the decay is a complicated process, with the rate of decrease becoming slower as the pressure falls from the initial high values (Wilson et al., 2019). On cessation of the shock impulse, the pressure signal sequence more gradually shows a negative pressure.

This "negative pressure phase" corresponds to the decreasing pressure within an expanding bubble of gaseous by-products of the explosive material that occur in the wake of the shockwave. The bubble expansion causes the pressure to

Figure 2. *Pressure signal from a Mk64 (**top**) and Mk82 (**bottom**) SUS charge measured by a hydrophone suspended 20 m below the surface.* ***Red lines:*** *reflection from the sea surface.*

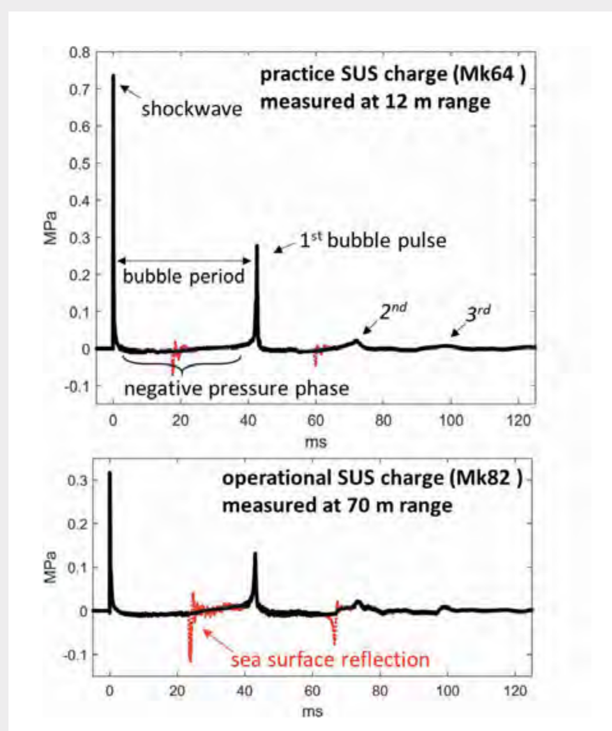

match and briefly go below the hydrostatic pressure, forcing a rapid collapse that produces a second sharp impulse. The collapse and rebound cycle of the gas bubble generates a series of "bubble pulses" that are a hallmark of underwater explosions. It is this bubble pulse series that generates the high signal energy at low frequencies.

This brief summary of the characteristics of an underwater explosion provides a rough introduction. Some additional details are now provided on the two hallmark features of an underwater explosion: the scaling law governing peak acoustic pressure relative to explosive weight and the properties of the bubble pulse.

Scaled Range Theory and Long-Range Propagation

The peak pressure levels one would experience when hearing an explosion depend primarily on two things: (1) how far away the receiver is from the explosion and (2) the total explosive weight. Moreover, the peak acoustic pressure levels from an explosion follows an important scaling law (Chapman, 1985), discovered over a century ago. This scaling law shows that peak pressure levels of the shockwave follow a function of range divided by the cube root of the explosive weight (i.e., scaled range). Scaling constants have been derived from a vast set of empirical measurements, made at a very close distance and at some distance from charges of varying weights, to establish the accurate predictions of peak pressure for many types of explosives. Thus, with scaled range, one can predict the peak pressure of the shock impulse emanating from an underwater explosion.

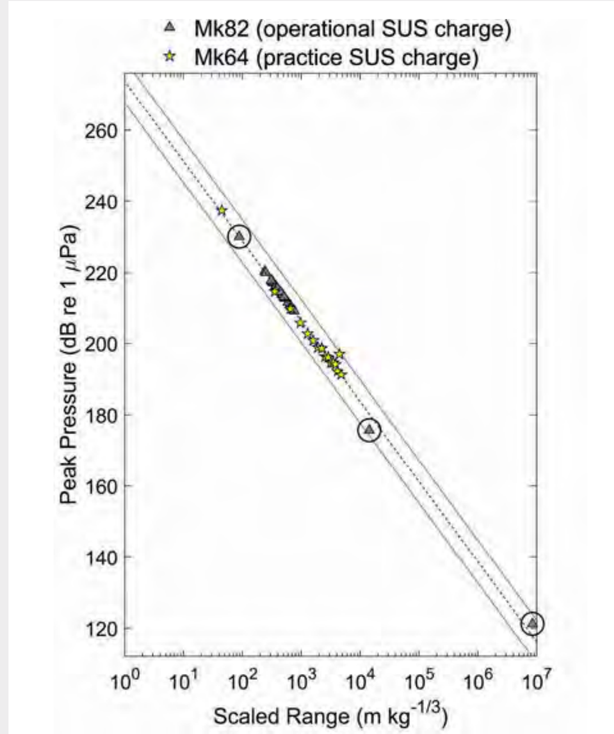

Figure 3. *Measurements of peak pressure from operational SUS charges (**gray triangles**) and practice SUS charges (**yellow stars**), shown as a function of scaled range. Near the source, the peak pressure levels follow scaled range predictions (**dashed line**) and fall within ±6 dB out to 10 km. **Open circles:** simultaneous measurement of the Mk82 charge shown in **Figure 2** at three locations, including a hydrophone station over 8,000 km away.*

Although there is a limit of validity for scaled range, the relationship seems to be surprisingly robust. **Figure 3** shows the peak pressure of SUS charges as a function of scaled range. These include measurements of operational SUS charges (**Figure 3**, *gray triangles*) made in deep water (Chapman, 1985) at short enough ranges where the reflections from the sea surface or seafloor do not interfere with the direct (shortest) path, and measurements of practice SUS charges (**Figure 3**, *yellow stars*) made in shallower water (75 m deep) where multiple echoes from the sea surface and seafloor can interfere, causing a deviation from the scaled range theoretical curve. As expected, the peak pressures follow the scaled range law (**Figure 3**, *dashed line*) and deviate only at long ranges where the echo interference is inevitable (and at most only 2 times, or 6 dB, the predicted level). Perhaps to some surprise, the operational SUS (**Figure 2**, *bottom*) was also measured 8,000 km away, with a peak pressure of about 1 Pa, which coincidently matches the prediction from scaled range theory (**Figure 3**, *open circles*).

The Bubble Pulse and Effect of Detonation Depth Below the Water Surface

The sequence of events following an underwater detonation reveals a spherical globe of gas growing outward from the point of detonation. This void in the water is filled with water vapor and the vaporized by-products of the explosive material, which, for conventional explosives, are chiefly carbon and nitrous oxides (Keevin and Hempin, 1997). The inertia of the expanding globe creates a low-pressure bubble that expands to a maximum radius, which if large enough may break the surface and vent the gases into the atmosphere. However, if the explosion is deeper, the bubble stops growing due to the opposing force of the surrounding ocean, and it is rapidly recompressed. The inward inertia overshoots equilibrium, compressing the gas bubble to a significant pressure that generates a second strong sound pulse. The time between the shock wave and this first bubble pulse is referred to as the bubble period.

After the first bubble pulse, the repeated collapse and rebound continues for several more cycles. Each time the cycle repeats, an additional sound pulse is generated, with diminishing peak pressures because the gas volume loses energy during the oscillations. The bubble rises vertically in the water throughout its series of oscillations, like a rising balloon, and subsequent bubble pulses originate from shallower depths than the detonation depth.

The twin impulses in the explosive charge signal (shockwave + first bubble pulse) establish a feature in the spectrum of the sound source that persists as it propagates, even when the signal is compounded with many echoes and becomes highly dispersed. The acoustic signal thus has encoded within it information about the properties of the explosion, specifically, the explosive weight and detonation depth. Thus, this bubble pulse feature is a unique identifier of an explosion, one that assists in its detection across ocean basins (Dall'Osto, 2019) and in discriminating explosions from the other impulses in ocean noise like tsunami-generating earthquakes (Simons et al., 2021).

A simple relationship exists for predicting the bubble period, following the same scaling by the cube root of the explosive weight as the scaled range. This is particularly useful when trying to identify an unknown explosion, from which one can infer its magnitude and depth. Revisiting the SUS data to demonstrate this application, even though the operational SUS charge has 26 times more explosive than the practice charge, it detonated 5 times deeper, resulting in bubble pulse signals from these 2 SUS charges that are remarkably similar (both signals have a sharp bubble pulse peak at 42 ms; see **Figure 2**).

We can also gather the size of the bubble created by the explosion from these same empirical curves. The practice SUS charge, which detonated at an 18-m depth, produced an 84 cm diameter bubble. The operational charge detonated 5 times deeper than the practice charge and produced a bubble twice that in diameter (1.6 m). Even though the larger operational SUS charge generated a bigger bubble, the greater hydrostatic pressure collapsed it in the same time as the smaller bubble of the practice charge at its shallower depth.

In comparison to the near instantaneous rise in pressure for the shock pulse, a closer inspection of the bubble pulses in **Figure 2** shows that the rise times to the peak pressures are gradual (a few milliseconds compared with less than a microsecond). Moreover, the rise and decay times of the bubble pulses are not symmetrical due to the energy loss during the cycle. **Figure 2** also demonstrates that the periods between sequential bubble pulses and their amplitudes both decrease. Interestingly, the explosions of these SUS charges were totally contained in the ocean with no visible disturbance on the sea surface. However, if either explosion were much shallower (say within a few bubble radii), its bubble could break the surface and burst, abruptly ending the bubble pulse sequence. This doesn't generally happen with SUS charges, which are small enough and detonate deep enough that their bubble remains totally contained underwater.

The scaled relationships for the bubble size are also useful in determining what "type of surface eruption" will be observed (**Figure 4**, *right*), which compounds and grows with each bubble pulse. **Figure 4** shows a photo of the surface phenomena from a 4.7-kg underwater explosion detonated at a 10-m depth; the accompanying table details the types of surface phenomenon expected for a detonation depth in terms of the maximum radius of its gas bubble. This explosion produced a roughly 4-m-diameter bubble, so at a 10-m depth, the surface above the explosion appears as a mound of frothy water (its whiteness caused by the cavitation of the water under the extreme pressures). The reflection of the bubble pulses from the sea surface can be observed in the surface eruption, each bubble pulse sending plumes of water jetting through the cavitation layer.

Considerations and Applications

Effect of Reflections

Underwater shockwaves from an explosion will eventually encounter and reflect from boundaries, although the effect of the sea surface and seabed are starkly different. The sea surface, which is a pressure release boundary,

detonation depth (in bubble radii)	type of surface eruption
> 40	total containment
25 – 40	upwelling
7 – 25	mounds
4 – 7	mounds developing into plumes
1 – 4	ring of plumes
0.2 – 1	column with central jet
< 0.2	column with smoke crown

Figure 4. ***Left:*** *photo sequence of the surface eruption from a 4.7-kg explosion at a 10-m depth, taken off San Diego, California. The white froth on the surface is a cavitation layer generated by the intense pressures, and water erupting out of the layer is due to the bubble pulse series.* ***Right:*** *accompanying table (Mellor, 1986) predicting the surface expression for any sized explosion based on the detonation depth relative to the radius of its gas bubble. Photo from 2018 LMR Field Team.*

cancels the incident energy of the shockwave, producing a reflected echo that is a negative copy of the shockwave. As discussed with respect to **Figure 4**, there is a limit as to how large the negative peak pressures can be because cavitation sets in when pressure drops below the atmospheric pressure.

Reflections from the seafloor depend on the sediment composition and, importantly, the angle at which the shockwave reflects from the seafloor. At steep angles of incidence (i.e., near vertical), only a fraction of the energy is reflected, thereby reducing the amplitude from scaled range predications. At shallow reflection angles, particularly angles less than the critical angle, where this angle is defined as $\cos^{-1}(c_w/c_b)$, where c_w and c_b are seawater and seabed sound speeds, respectively, the reflected amplitude is much higher.

These effects are illustrated in **Figure 5** using pressure waveform data measured at 28 m and 68 m from an explosive source in waters of approximately 20 m in depth. The data originate from a study (Dahl et al., 2020) examining the effects of underwater explosions on fish (see ***Conserving Marine Life***). A 7-ms period for each graph contains the arrival of the primary shockwave (**Figure 5**, *number 1*) and a reflection from the sea surface (**Figure 5**, *number 2*) and seafloor (**Figure 5**, *number 3*). Well beyond this period (not shown), the waveforms contain the arrival of the first, second, and, in some cases, a third bubble pulse. These are observed at successive delays of about 250 ms, as predicted for an explosive charge at this depth (about 10 m) and equivalent weight of 4.7 kg of TNT (see **Figure 4**).

At a range of 28 m (**Figure 5**, *top*), the maximum observed peak pressure of the shockwave is 247 dB re 1 μPa (**Figure 5**, *number 1*), which is well predicted by the scaled range theory given the weight of explosive charge. The bottom reflection (**Figure 5**, *number 2*) arrives about 4 ms later, and its amplitude is reduced by about 40%. The reflection angle is about 35°, which is greater than the critical angle for this seabed, explaining the significant reduction in amplitude. Following this arrival (approximately 1 ms later), the surface-reflected path (**Figure 5**, *number 3*) arrives that causes an abrupt reduction in pressure. The

Figure 5. ***Top:*** *acoustic pressure (in MPa) versus time measured at range of 28 m from the source. Key features of the times (**1, 2, 3**) correspond to the arrival of the direct path, bottom-reflected path, and sea surface-reflected path, respectively. The onset of cavitation from the sea surface is indicated by the highly oscillatory behavior of the sea surface-reflected path that averages approximately −100 kPa.* ***Solid and dotted lines:*** *0 kPa and −100 kPa reference lines, respectively.* ***Bottom:*** *same as above but measured at a range of 68 m. Adapted from Dahl et al., (2020), with permission of Acoustical Society of America. © 2020, Acoustical Society of America.*

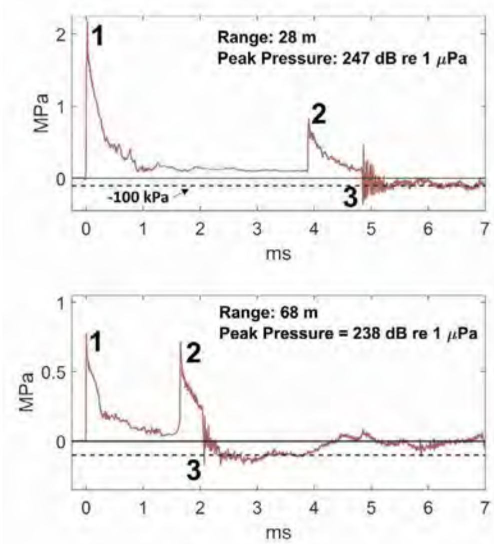

sequence of sharp spikes at **Figure 5**, *number 3*, the first of which is negative, identifies the leading edge of the surface-reflected pulse before the onset of cavitation (Wentzell et al., 1969) during which the waveform reaches an approximate average value of about −100 kPa, indicative of cavitation.

At a range of 68.5 m (**Figure 5**, *bottom*), the maximum observed peak pressure is 238 dB re 1 μPa. The sequence of arrivals (**Figure 5**, *numbers 1-3*) is compressed owing to the longer range; **Figure 5**, *numbers 1-2*, is now closer in amplitude that might be anticipated given the grazing angle of ~18°, which is less than the critical angle. The surface echo (**Figure 5**, *number 3*) arrives about 0.5 ms after the bottom reflection (**Figure 5**, *number 2*) and represents an excellent example of the cavitation surface cutoff effect, and, in this case, the expected cavitation amplitude of about −100 kPa is more easily seen.

Measuring Sediment Properties

The shockwave of a SUS charge provides an effective signal to study the structure of the seabed and its stratigraphy, the layers of distinct sediment formed over millennia. The stratigraphy of a continental shelf contains valuable information relating to the geological processes and climatic history. SUS charges are powerful enough to propagate sound through kilometers of sediment, echo off bedrock below and back into the water column. Stratigraphy can be interpreted from the echoes, and geoacoustic parameters (density, sound speed, and attenuation) are inverted to identify layers of different media.

One recent example of the use of a SUS charge is in the US Office of Naval Research's Seabed Characterization Experiment (SBCEX), an ongoing series of field experiments focused on a large patch of seabed with a thick layer of mud, roughly 100 km south of Martha's Vineyard, Massachusetts. Marine mud has a unique geoacoustic property that renders it almost acoustically transparent except at low angles (Ballard and Lee, 2017). Importantly, the broadband shockwave from an SUS charge provides the necessary bandwidth to identify the layering structure within the mud, layers that have been deposited over thousands of years spanning multiple ice ages.

Figure 6 shows a zoomed-in view of the shockwave from an Mk64 (**Figure 6**, *gray line*) and its low-angle bottom reflection from the muddy seabed reflection (**Figure 6**, *black line*). Note how the bottom reflection appears modulated at a particular frequency (its period [*T*] is annotated in **Figure 6**). This modulation is attributed to the trapping of specific frequencies in a low-speed sound channel formed in the upper layers of the muddy seabed (Dall'Osto and Tang, 2022). Inversions of SUS charge data like this, taken along with the stratigraphy as determined by prior seismic surveys of the mud patch, have identified the spatial dependence of the mud geoacoustic properties (Knobles et al., 2020), which provide insight into the physical processes that have led to this large deposit that supports a thriving lobster fishery.

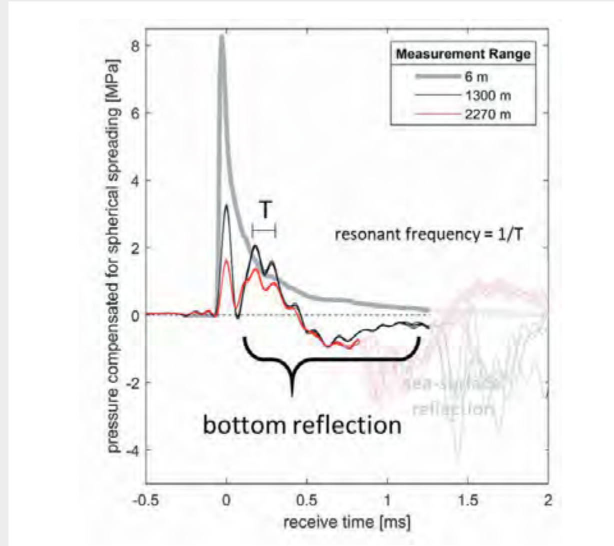

Figure 6. *A zoomed-in view of the shockwave from a Mk64 SUS shockwave (**gray line**), and the waveform recorded 1.1 m above the seafloor at a range 1.30 km from the explosion (**black line**) and at 2.27 km (**red line**). The signal levels have been corrected by the spherical spreading (i.e., multiplied by the respective range). In the bottom-reflected signal, the sediment layering imparts a modulation, annotated by its characteristic timescale (*T*). Adapted from Dall'Osto and Tang (2022).*

Conserving Marine Life

Underwater explosions are occasionally necessary for activities such as demolishing derelict oil rigs or wind farm pilings, marine construction, and military training. The great body of work developed to understand sound propagation from SUS charges has created the predictive measures that apply to nearly all explosions. These relationships even apply to the charges used to protect fish stocks from marine mammals, called "seal bombs"

(Wiggins et al., 2021) that are small waterproof firecrackers used, for example, to scare away sea lions looking for an easy meal of salmon waiting to jump through the fish ladder on a dammed river.

The use of underwater explosions, however, requires a careful consideration about their potential effects on marine life. Much like the protocols for using large explosives in demolition and mining, a safety perimeter around the detonation site is monitored to minimize impact on marine life.

For example, the US Navy at-sea training activities involving underwater explosive charges, the use of which must comply with a suite of US federal environmental laws and regulations to protect marine life. However, almost nothing is known about the potential effects of explosions on fishes (nor on marine invertebrates). Thus, two of the authors (Dall'Osto and Dahl along with *Acoustics Today* editor Arthur Popper) have been involved in a project to conduct field-based experiments on the effects of underwater explosions on fishes. The goal is to examine explosive effects on fish species with differing anatomical characteristics (e.g., swim bladder morphology) and size at varied water depths and distances from the source. Such data are needed to develop guidelines and threshold criteria for the effects on fish resulting from exposure to underwater explosives. The results will help predict potential effects that may occur during Navy training activities.

Among the several acoustic measures, peak sound pressure expressed in decibels has emerged as an important a key predictor of severe internal tissue injury as result of exposure to an underwater explosion (Dahl et al., 2020; Jenkins et al., 2022; Smith et al., 2022). Scaled range clearly helps to predict the distance animals need to be away from a particular explosive, although figuring out how many are too close is not always easy to determine for submerged animals.

Underwater Explosions and the Future of Marine Research

Early underwater acoustic research relied on underwater explosions as sources of sound. The unique high-source level and broadband nature (covering both low and high frequencies) of underwater explosions are invaluable for current research efforts. The existing stockpile of SUS charges still enables research, from probing the earth's structure deep under the oceans to rapidly characterizing the ocean's temperature distribution to identify the anomalies that fuel tropical storms. Balancing what we know about the danger from underwater explosions, including the ranges required to minimize their impact, small SUS charges can be used responsibly to provide answers to some very difficult questions.

References

Ballard, M. S., and Lee, K. M. (2017). The acoustics of marine sediments. *Acoustics Today* 13(3), 11-18.

Chapman, N. R. (1985). Measurement of the waveform parameters of shallow explosive charges. *The Journal of the Acoustical Society of America* 78, 672-681. https://doi.org/10.1121/1.392436.

Dahl, P. H., Jenkins, A. K., Casper, B., Kotecki, S. E., Bowman, V., Boerger, C., Dall'Osto, D. R., Babina, M. A., and Popper, A. N. (2020). Physical effects of sound exposure from underwater explosions on Pacific sardines (*Sardinops sagax*). *The Journal of the Acoustical Society of America* 147, 2383-2395. https://doi.org/10.1121/10.0001064.

Dall'Osto, D. R., (2019). Taking the pulse of our ocean world. *Acoustics Today* 15(4), 20-28. https://doi.org/10.1121/AT.2019.15.4.20.

Dall'Osto, D. R., and Tang, D. (2022). Acoustic resonances within the surficial layer of a muddy seabed. *The Journal of the Acoustical Society of America* 151, 3473-3480. https://doi.org/10.1121/10.0011472.

Jenkins, K. A., Dahl, P. H., Kotecki, S. E., Bowman, V., Casper, B., Boerger, C., and Popper, A. N. (2022). Physical effects of sound exposure from underwater explosions on Pacific mackerel (*Scomber japonicus*): Effects on non-auditory tissues. *The Journal of the Acoustical Society of America* 151, 3947-3956. https://doi.org/10.1121/10.0011587.

Keevin, T. M., and Hempen, G. L. (1997). *The Environmental Effects of Underwater Explosions with Methods to Mitigate Impacts*. Prepared for the Office of the Chief of Engineers, US Army Corps of Engineers, St. Louis District, St. Louis, MO. Available at https://apps.dtic.mil/sti/citations/ADA575523.

Knobles, D. P., Wilson, P. S., Goff, J. A., Wan, L., Buckingham, M. J., Chaytor, J. D., and Badiey, M. (2020). Maximum entropy derived statistics of sound-speed structure in a fine-grained sediment inferred from sparse broadband acoustic measurements on the New England continental shelf. *IEEE Journal of Oceanic Engineering* 45, 161-173. https://doi.org/10.1109/JOE.2019.2922717.

Mellor, M. M. (1986), *Blasting and Blast Effects in Cold Regions. Part II: Underwater Explosions*, Special Report 86-16 prepared for the Office of the Chief of Engineers, US Army Cold Regions Research and Engineering, Hanover, NH. Available at https://apps.dtic.mil/sti/pdfs/ADA178363.pdf.

Muir, T. G., and Bradley, D. L. (2016). Underwater acoustics: a brief historical overview through World War II. *Acoustics Today* 12(3), 40-48.

Schulze, J. N., Denkinger, J., Oña, J., Poole, M. M., and Garland, E. C. (2022). Humpback whale song revolutions continue to spread from the central into the eastern South Pacific. *Royal Society Open Science* 9, 220158. https://doi.org/10.1098/rsos.220158.

Simons F. J., Simon, J. D., and Pipatprathanporn, S. (2021). Twenty-thousand leagues under the sea: Recording earthquakes with autonomous floats. *Acoustics Today* 17(2), 42-51. https://doi.org/10.1121/AT.2021.17.2.42.

Smith, M. E., Accomando, A. W., Bowman, V., Casper, B. M., Dahl, P. H., Jenkins, A. K., Kotecki, S., and Popper, A. N. (2022). Physical effects of sound exposure from underwater explosions on Pacific mackerel (*Scomber japonicus*): Effects on the inner ear. *The Journal of the Acoustical Society of America* 152, 733-744. https://doi.org/10.1121/10.0012991.

Wentzell, R. A., Scott, H. D., and Chapman, R. P. (1969). Cavitation due to shock pulses reflected from the sea surface. *The Journal of the Acoustical Society of America* 46, 789-794. https://doi.org/10.1121/1.1911762.

Wiggins, S. M., Krumpel, A., Dorman, L. M., Hildebrand, J. A., and Baumann-Pickering, S. (2021). Seal bomb explosion sound source characterization. *The Journal of the Acoustical Society of America* 150, 1821-1829. https://doi.org/10.1121/10.0006101.

Wilson, P. S., Knobles, D. P., Dahl, P. H., and McNeese, A. R. (2019). Short-range signatures of explosive sounds in shallow water used for seabed characterization. *IEEE Journal of Oceanic Engineering* 45, 161-173. https://doi.org/10.1109/JOE.2019.2934372.

Contact Information

David R. Dall'Osto
dallosto@uw.edu

Applied Physics Laboratory
University of Washington
1013 NE 40 Street
Seattle, Washington 98105, USA

Peter H. Dahl dahl97@uw.edu

Applied Physics Laboratory
University of Washington
1013 NE 40 Street
Seattle, Washington 98105, USA

N. Ross Chapman
chapman@uvic.ca

School of Earth and Ocean Sciences
University of Victoria
PO Box 1700 STN CSC
Victoria, British Columbia V8W 2Y2, Canada

For author bios, please go to acousticstoday.org/bios-19-1-1